Biochemistry and Biophysics Reports 30 (2022) 101242

Contents lists available at ScienceDirect

Biochemistry and Biophysics Reports

journal homepage: www.elsevier.com/locate/bbrep

Sequence-specific destabilization of azurin by tetramethylguanidinium-dipeptide ionic liquids

Roshani Patel, Austin K. Clark, Gabriella DeStefano, Isabella DeStefano, Hunter Gogoj, Erin Gray, Aashka Y. Patel, Joshua T. Hauner, Gregory A. Caputo, Timothy D. Vaden *

Department of Chemistry and Biochemistry, Rowan University, Glassboro, NJ, 08028, USA

ARTICLE INFO

Keywords:
Ionic liquids
Azurin
Protein stability
Dipeptides

ABSTRACT

The thermal unfolding of the copper redox protein azurin was studied in the presence of four different dipeptide-based ionic liquids (ILs) utilizing tetramethylguanidinium as the cation. The four dipeptides have different sequences including the amino acids Ser and Asp: TMG-AspAsp, TMG-SerSer, TMG-SerAsp, and TMG-AspSer. Thermal unfolding curves generated from temperature-dependent fluorescence spectroscopy experiments showed that TMG-AspAsp and TMG-SerSer have minor destabilizing effects on the protein while TMG-AspSer and TMG-SerAsp strongly destabilize azurin. Red-shifted fluorescence signatures in the 25 °C correlate with the observed protein destabilization in the solutions with TMG-AspSer and TMG-SerAsp. These signals could correspond to interactions between the Asp residue in the dipeptide and the azurin Trp residue in the unfolded state. These results, supported by appropriate control experiments, suggest that dipeptide sequence-specific interactions lead to selective protein destabilization and motivate further studies of TMG-dipeptide ILs.

1. Introduction

Ionic liquids (ILs, liquid salts composed of an organic cation and an organic or inorganic anion [1]) have been broadly studied for their material properties and electrochemical applications of ILs. More recent studies have begun to search for biocompatible ILs [2–5]. ILs have found a broad variety of applications in biomedicine and biomedical technologies [6–14], including many different protein applications [15–20]. The past ~10 years have seen a dramatic increase in studies of ionic liquids (ILs) and their effects on protein structures and stabilities [7,17,21–25].

One of the most attractive aspects of ILs from the applications standpoint is the wide variety of molecular cation-anion pairs available for IL design. These numerous combinations allow for sampling significant amounts of chemical space and provide the basis for developing tunable ILs in which the molecular ions are chosen for particular biomolecular functions. Amino acid ILs (with the amino acid as anion) [26–29] offer many options for selective and tunable biocompatible ILs for a variety of biomedical/biotechnology applications. Similarly, the tetramethylguanidine (TMG) cation has been proposed as a suitable component for biomolecular interactions [30,31]. The IL TMG-acetate stabilizes H-bonding in DNA [32], TMG-lactate destabilizes the β-sheet structure in silk proteins [24], and our group has reported side-chain specific destabilization effects on the β-barrel protein mCherry by two different TMG-amino acid ILs [33].

Numerous proteins have been characterized with ILs including silk fiber proteins, keratin, collagen, laccase, lysozyme, myoglobin, and many others [34–39]. Recent studies have focused on metalloproteins [16]. Our group reported the first two studies on the bacterial redox protein azurin in ILs [31,40]. While azurin is found in many bacterial strains, the *Pseudomonas aeruginosa* azurin is by far the most thoroughly studied form. In cells, azurin serves as an electron transfer protein as part of the electron transport chain involved in the dentirification process in *P. aeruginosa* [41–43]. Electron shuttling is achieved through the use of a copper ion bound to the azurin protein structure [44], which contains both an α-helix and a small β-barrel [45]. Azurin has been a protein of interest for many groups since it exhibits the most blue-shifted Trp emission spectrum of any known protein (~308 nm) [46–48] arising from a single Trp residue buried in the interior of the β-barrel domain. It is also interesting as a redox protein that could be used in biotechnology applications focused on its denitrification function and potential uses in nitrate decontamination of water or soil [49–52].

Initial studies on azurin with imidazolium-based ILs demonstrated that IL cation hydrophobicity correlates with protein destabilization,

* Corresponding author. Department of Chemistry and Biochemistry Science Hall, Rowan University, Office 301K 201 Mullica Hill Rd. Glassboro, NJ, 08028, USA.
E-mail address: vadent@rowan.edu (T.D. Vaden).

https://doi.org/10.1016/j.bbrep.2022.101242
Received 18 January 2022; Received in revised form 18 February 2022; Accepted 2 March 2022

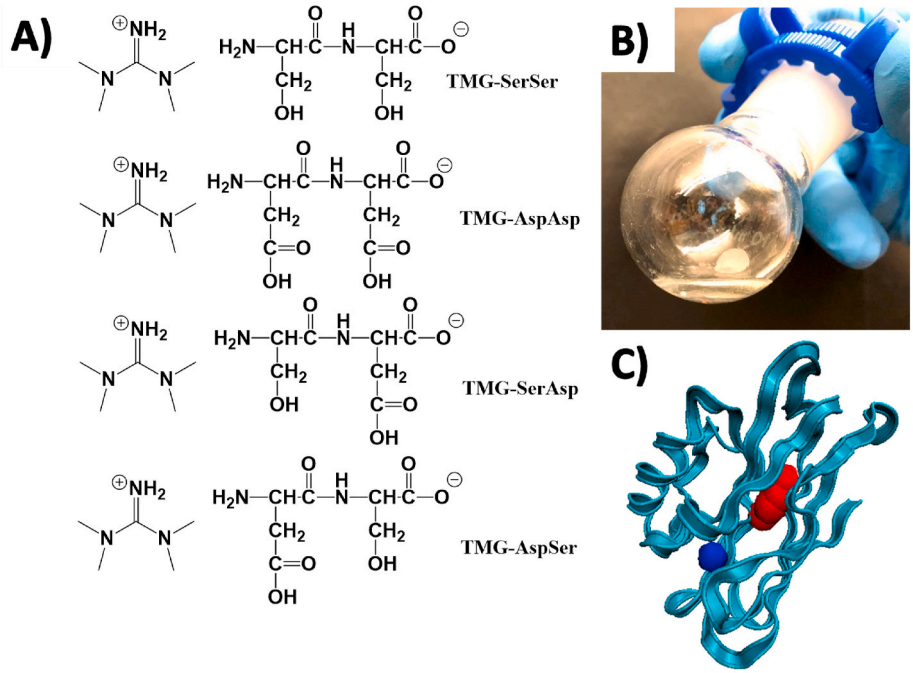

Fig. 1. A) Structures of TMG-dipeptide ILs used in this work; B) Photograph demonstrating the liquid nature of TMG-SerAsp, as an example; C) Structure of azurin [45] with the Trp residue highlighted in red. The Cu^{2+} is shown in blue. (For interpretation of the references to colour in this figure legend, the reader is referred to the Web version of this article.)

which is primarily driven by entropic effects [40]. TMG-amino acid ILs have selective destabilization effects, as revealed by thermodynamic measurements coupled with molecular dynamics simulations [31]. TMG-Ser and TMG-Thr, which have alcohol side chains, strongly destabilize azurin by increasing unfolding entropy while leaving unfolding enthalpy mostly unchanged [31]. In contrast, TMG-Asp and TMG-Glu, with acid side chains, have weaker destabilization effects because both unfolding entropy and enthalpy values are increased (hence, minor net changes in unfolding free energies) [31].

In this work we build on the previous studies of TMG-amino acid ILs and their effects on azurin by investigating azurin protein destabilization by TMG-dipeptide ILs. Four different dipeptides containing Asp and Ser were used to make four TMG-based ILs, TMG-AspAsp, TMG-SerSer, TMG-AspSer, and TMG-SerAsp, shown in Fig. 1. The results elucidate sensitive differences in how the different dipeptide sequences affect the azurin protein structure and suggest sequence-specific selectivity in azurin-protein interactions.

2. Experimental methods

2.1. Azurin expression and purification

Azurin expression and purification was carried out as described previously [31,40]. In summary, *Escherichia coli (E. coli)* was transformed by using a plasmid expressing azurin from *P. aeruginosa* and a kanamycin selectable marker (Genscript, Piscataway, NJ). Bacterial colonies were grown on a kanamycin LB-agar plate. Colonies from this plate were then chosen to be grown in an LB broth, which contained 1 mg/L of copper sulfate and 80 mg/L magnesium sulfate. To induce expression, isopropyl β-D-1-thiogalactopyranoside (IPTG, Alfa Aesar) was added to the broth to a final concentration of 1 mM. These cells were centrifuged and frozen before the protein purification procedure. For protein extraction, cells were lysed via sonication in a buffer containing ethylenediamine tetraacetic acid, sucrose and lysozyme. After centrifugation, acid precipitation in pH 4.1 ammonium acetate buffer was performed followed by column chromatography with a CM sepharose column. Copper (II) chloride was added to the protein-containing fractions and a second pH gradient column chromatography procedure was performed with a CM sepharose column. The fractions containing azurin were dialyzed overnight and then lyophilized. Azurin purity was confirmed by fluorescence and IR spectroscopy. Gel electrophoresis and UV absorbance measurements were also performed on fractions from the second column procedure and are shown in Figure S1 and Figure S2 for chromatographic characterization.

2.2. TMG-dipeptide IL synthesis and purification

Tetramethyl guanidine (99%) was purchased from Tokyo Chemical Industry and used without further purification. Serine-serine dipeptide, aspartic acid-aspartic acid dipeptide, and serine-aspartic acid dipeptide were purchased from Bachem AG and used without further purification. Aspartic acid-serine dipeptide was purchased from GeneScript and used without purification. To synthesize the TMG-dipeptide ILs, TMG and the dipeptide were mixed together in distilled water in a 1:1 molar ratio under nitrogen gas purge. The mixture stirred for 45 min under nitrogen, followed by 30 min without nitrogen. Vacuum evaporation at ~50 °C was used to remove the water. About 300 μL of each IL was made. The liquid nature is confirmed in Fig. 1A.

TMGHCl, containing protonated TMG and the chloride anion, was synthesized by mixing TMG with 1.0 M HCl in 1:1 molar ratios followed by vacuum evaporation.

2.3. Sample preparation and fluorescence spectroscopy

1.0 M stock IL solutions were prepared in distilled water from the pure ILs. All solutions of azurin with ILs were prepared with ~2 mg/mL azurin in distilled water. Control experiments were performed to investigate how pH and buffer presence/absence affected azurin thermal unfolding. These control experiments were performed with 20 mM pH 4 sodium acetate buffer, 20 mM pH 7 sodium phosphate buffer, and 20 mM pH 10 ammonium buffer. All samples were measured within a few hours after preparation.

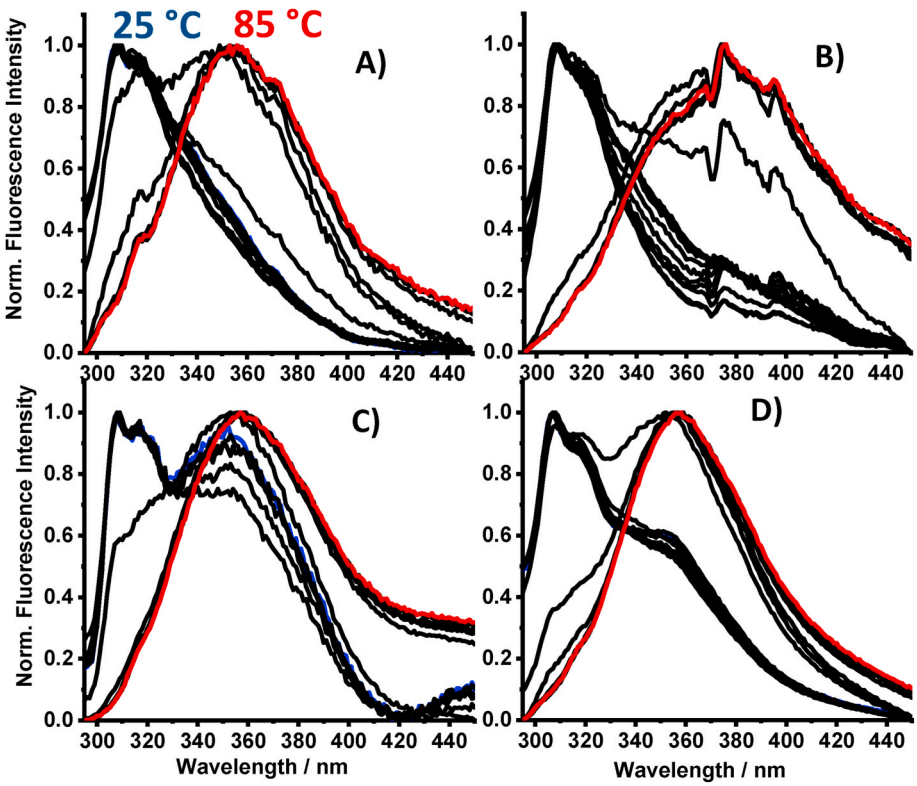

Fig. 2. Normalized fluorescence spectra for TMG-dipeptide ILs with increasing temperature. The peak at 308 nm corresponds to folded azurin and the peak at 355 nm corresponds to unfolded azurin. In all sub-figures, the lowest-temperature trace is blue, the highest-temperature trace is red, and all other traces are black. (A) TMG-AspAsp; (B) TMG-SerSer; (C) TMG-SerAsp; (D) TMG-AspSer. (For interpretation of the references to colour in this figure legend, the reader is referred to the Web version of this article.)

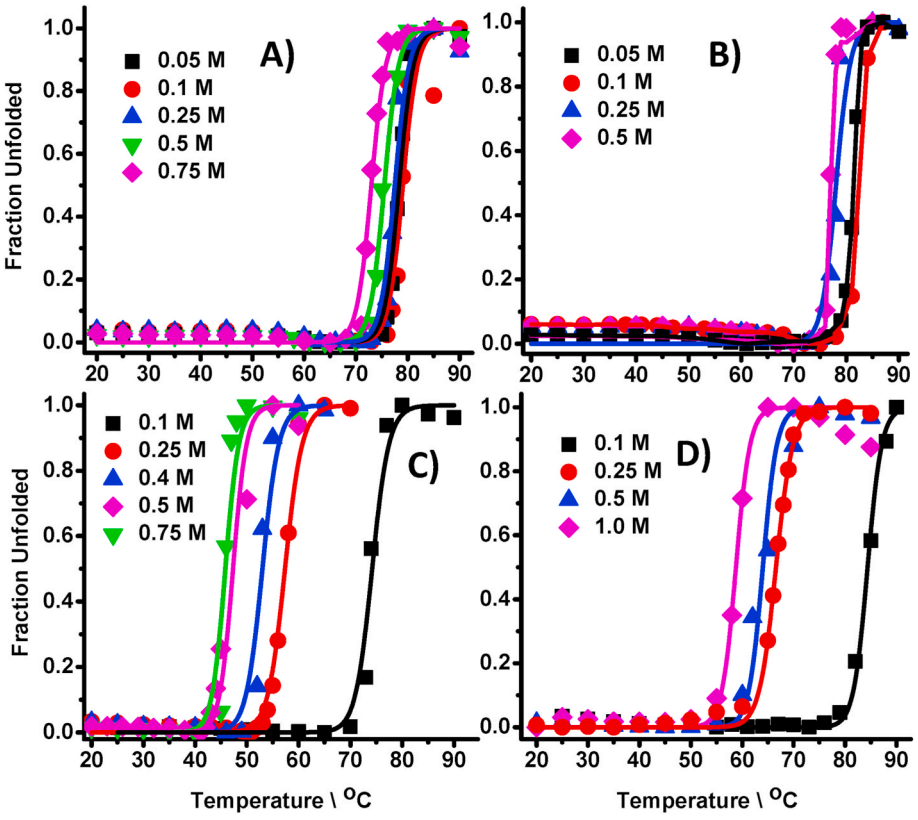

Fig. 3. Unfolded protein fraction plotted against temperature for TMG-dipeptide ILs with increasing concentration from 0.1 M to 0.75 M. The data points are computed using Equation (1) and the solid lines are fits to the data used only as guides. (A) TMG-AspAsp; (B) TMG-SerSer; (C) TMG-SerAsp; (D) TMG-AspSer.

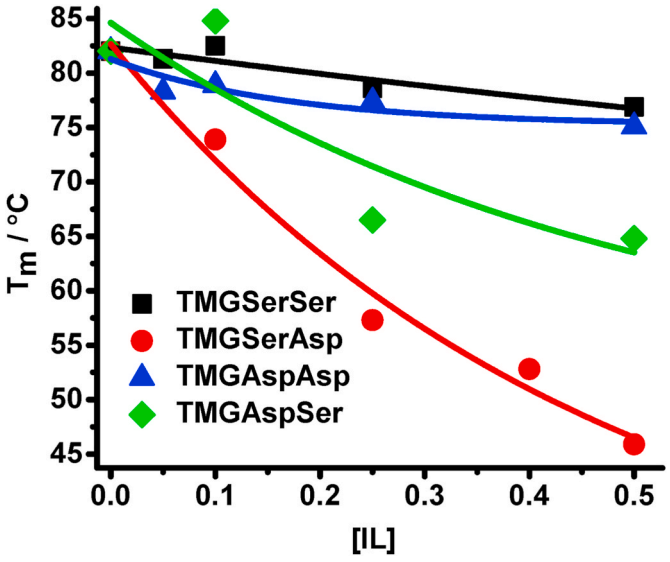

Fig. 4. Unfolding temperature (interpolated from Fig. 3) plotted against TMG-dipeptide IL concentration.

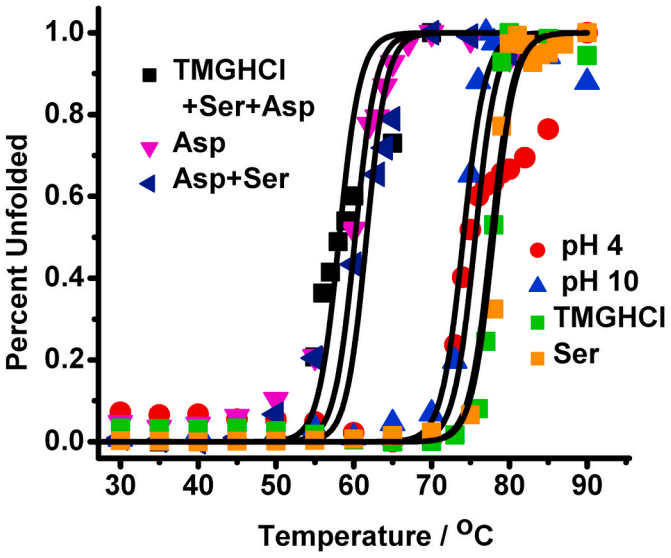

Fig. 5. Unfolding curves for control experiments. pH changes (performed by using different buffers), TMG^+ alone, and serine alone do not significantly destabilize azurin. However, mixtures containing free aspartic acid have strong destabilizing effects.

A Horiba FluoroMax 4 spectrofluorometer was used to record fluorescence spectra. All samples were excited at 285 nm, and emission spectra were recorded from 295 nm to 450 nm with 3 nm slit width. Spectra were recorded at temperatures from 20 °C to 90 °C using a Peltier-based temperature controller. From previous reports [31,40], the azurin fluorescence peak is at 308 nm when folded and at 355 nm when unfolded. For any temperature, the normalized unfolded protein fraction (F_u) can be calculated using the ratio of fluorescence intensities at 308 nm and 355 nm (I_{355}/I_{308}) [31]:

$$F_u = \frac{(I_{355}/I_{308}) - (I_{355}/I_{308})_{folded}}{(I_{355}/I_{308})_{unfolded} - (I_{355}/I_{308})_{folded}} \quad (1)$$

When necessary, fluorescence spectra were corrected for any signals arising from the ILs alone. However, for the most part the pure ILs (in solution) do not have strong fluorescence signals in the spectral region studied and any weak signals arise most likely from trace impurities in the commercial TMG or amino acid materials. Such signals are broad and much weaker than the azurin fluorescence signals and do not interfere with the results. Notably, Equation (1) corrects for weak IL-based fluorescence signals under the valid assumption that these are not strongly temperature dependent.

3. Results

The fluorescence spectra recorded at increasing temperatures for azurin in the presence of 0.5 M TMG-dipeptide ILs are summarized in Fig. 2. In each set of spectra, the transition from folded protein (with a peak at 308 nm) to unfolded protein (with a peak at 355 nm) can be clearly observed. Extra peaks in the TMG-SerSer data (Fig. 2B) around 360–400 nm arise from some impurity in the dipeptide. This impurity signal, which was not investigated beyond confirming that it arises from the commercial dipeptide, was subtracted from the fluorescence spectra but subtraction from the high-temperature fluorescence spectra did not fully remove the extra peaks. In the azurin spectra with TMG-SerAsp (Fig. 2C) and TMG-AspSer (Fig. 2D), fluorescence intensity is observed around 360 nm even in the room-temperature spectra. Notably the 308 nm peak at 308 nm is still present in all spectra below ~40 °C indicating that some population of azurin remains folded. The 360 nm peak is discussed later.

The thermal unfolding curves derived using Equation (1) from the data in Fig. 2 are shown in Fig. 3. Note that the simple unfolding analysis using Equation (1) is qualitatively unaffected by the presence of the 360 nm peak in the lower-temperature spectra with TMG-AspSer and TMG-SerAsp since the analysis relies on decreased 308 nm peak intensity to infer unfolding. The unfolding curve for azurin in water (with no IL) is not shown, but has been published and shows clear unfolding at 82 °C [31,40]. It is immediately clear from Fig. 3 that the TMG-AspAsp (Fig. 3A) and TMG-SerSer (Fig. 3B) do not significantly destabilize azurin while TMG-SerAsp (Fig. 3C) and TMG-AspSer (Fig. 3D) have some significant protein destabilizing effect. Hence, the mixed dipeptides destabilize the protein structure. It is also notable that the destabilization is stronger for TMG-SerAsp than for TMG-AspSer, which suggests some sequence-specific interaction. The melting temperatures, interpolated from Fig. 3 as the temperature at which half the protein is unfolded, are shown in Fig. 4 for azurin in the presence of the different ILs. The solid lines are exponential fits to the data used as a guide. The data in Fig. 4 is shown only up to 0.5 M IL concentration. As seen in Fig. 3, for some ILs data could be collected at higher IL concentrations (0.75 and 1.0 M), due to very low IL quantities some ILs could only be collected up to 0.5 M.

Fig. 4 shows protein melting temperatures (interpolated from the inflection points in Fig. 3) for azurin in the presence of the four different ILs. Fig. 4 quantitatively confirms the results of Fig. 3, as the ILs TMG-SerSer and TMG-AspAsp do not destabilize azurin while TMG-SerAsp and TMG-AspSer do destabilize azurin. This result for TMG-SerSer is especially interesting in the context of previous results that clearly show that TMG-Asp does not destabilize the azurin protein while TMG-Ser significantly destabilizes it. It is also interesting that the TMG-SerAsp and TMG-AspSer have clearly different effects on azurin. TMG-AspSer lowers the azurin melting temperature to ~65 °C while TMG-SerAsp lowers this value to below 45 °C. Clearly, the specific dipeptide sequence order is important for the degree of protein destabilization.

Important control data for understanding the results are summarized in Fig. 5. As noted above and in the literature [53], azurin unfolds at 82 °C in the absence of IL. Significantly changing solution pH from 4 to 10 (and in-between values, although data is not shown) has some minor destabilizing effect on azurin, but large changes in melting temperatures such as those observed in Fig. 4 are clearly not explained by solution pH changes alone.

Control experiments were performed with individual components of the ILs, all at 0.5 M. TMG^+, synthesized as TMGHCl, does not

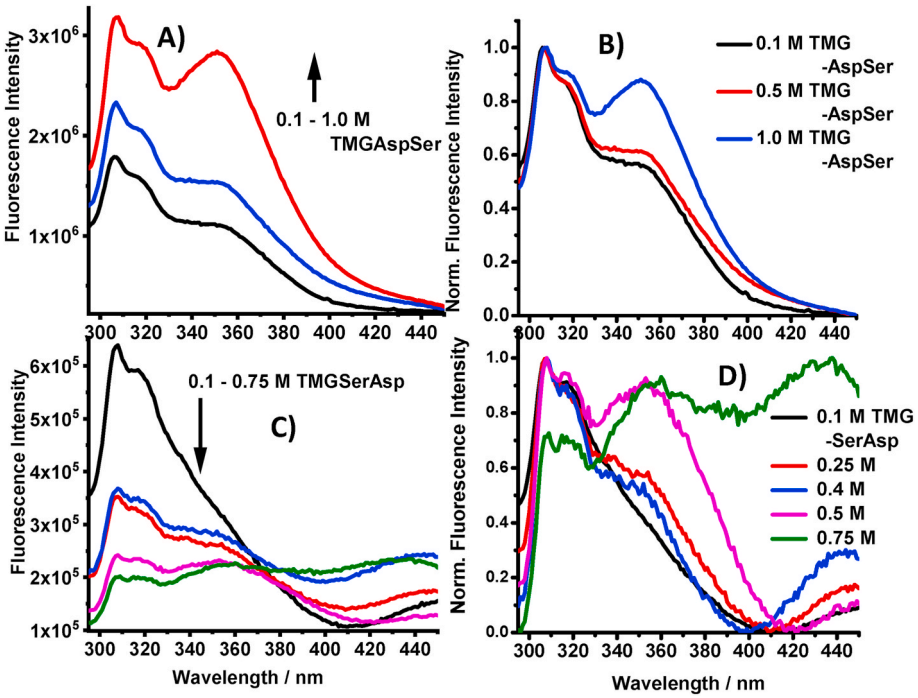

Fig. 6. Fluorescence spectra of azurin in the presence of increasing IL concentration for TMG-AspSer (A and B) and TMG-SerAsp (C and D). Both raw (A and C) and normalized (B and D) spectra are shown to illustrate fluorescence quenching effects (in raw spectra) and increasing relative intensity at 360 nm (in normalized spectra).

significantly destabilize azurin, and also serine alone has minimal effect on azurin (consistent with previous reports [40]). However, aspartic acid alone does significantly destablize azurin. Aspartic acid/serine mixtures and aspartic acid/serine/TMG^+ mixtures also destabilize azurin. Clearly, the Asp side chain has a significant role in destabilizing the azurin structure, but when incorporated into a dipeptide and combined with TMG^+ in the ILs, Asp may or may not affect the protein.

4. Discussion

Our results point to the sensitivity and selectivity in protein destabilization by TMG-dipeptide ILs. Previous results showed that TMG-Ser destabilizes azurin while TMG-Asp does not [31], which is attributable to a competitive balance between the TMG-protein and amino acid-protein interactions, also observed in studies of mCherry with TMG-Amino Acid ILs [33]. In the current work, TMG-AspAsp and TMG-SerSer do not significantly destabilize azurin but the mixed-residue TMG-dipeptide ILs (TMG-AspSer and TMG-SerAsp) have strong destabilization effects.

Clues regarding the nature of the TMG-dipeptide-protein interactions can be observed in the azurin fluorescence spectra with TMG-AspSer and TMG-SerAsp, summarized in Fig. 6. As mentioned in Section 3, red-shifted fluorescence signals are observed in the 25 °C spectra for azurin with TMG-AspSer (Fig. 6A and B) and TMG-SerAsp (Fig. 6C and D). These spectra show that the 360 nm peak increases in intensity with increasing concentration, but leaving the 308 nm peak (which corresponds to folded azurin) unaffected. Since azurin has only a single Trp residue (Fig. 1C), this indicates that with TMG-AspSer and TMG-SerAsp two protein structural populations exist: one in which the Trp remains buried in the β-barrel (that is, with folded protein) and one in which the Trp is in a different environment. Based on the analysis in Section 3 using Equation (1), the folded protein is strongly destabilized, and Fig. 6 suggests that the presence of the other population correlates with protein destabilization.

The spectra in Fig. 6 also show how the ILs quench the azurin fluorescence. Protein fluorescence quenching by ILs has been noted previously [54,55] and can highlight direct protein-IL interactions. While we have not pursued quantitative fluorescence quenching analysis yet, it does appear that the azurin – TMG-SerAsp interaction may be stronger than the azurin –TMG-AspSer interaction on the basis of stronger quenching (by TMG-SerAsp).

The nature of the structures in the protein conformational population giving rise to the 360 nm Trp fluorescence peak in Fig. 6 is unclear. Literature reports have detailed how interactions between tryptophan residues and aspartic acid can lead to red-shifted tryptophan fluorescence [56–58]. It is possible that the 360 nm fluorescence signals arise from specific Trp-Asp interactions, in which the dipeptide would penetrate into the azurin β-barrel, although this is unlikely since the barrel is tightly packed without a water core. Alternatively the signals could simply arise from unfolded protein structures, or unfolded structures in which the Trp interacts with Asp in the dipeptide. While it is difficult to distinguish these possibilities, the latter explanation is consistent with the results in Fig. 5. Trp-Asp interactions in the unfolded protein state would decrease the energy of the unfolded protein, thereby decreasing the unfolding enthalpy and the melting temperature.

Notably, 360 nm signals are absent in the azurin fluorescence spectra with TMG-AspAsp and TMG-SerSer (Fig. 2) and also absent in published results with TMG-Asp [31]. Taken together, the results of this current study highlight the sensitivity to exact dipeptide sequence in protein destabilization. The specific molecular mechanism for protein destabilization needs to be further investigated with simulations and more sensitive experiments, but clearly different dipeptide sequences have different effects on the protein structure and stability. This points to the value and possibilities for dipeptide-based ILs as specific, tunable biomaterials for protein applications.

5. Conclusions

In this work we have shown that different Asp/Ser sequences in TMG-dipeptide ILs have significantly different effects on the stability of the copper redox protein azurin. The TMG-AspAsp and TMG-SerSer ILs only weakly destabilize the protein, while the TMG-AspSer and TMG-

SerAsp ILs strongly destabilize the protein. Notably the TMG-SerAsp IL appears to interact more strongly with azurin (relative to TMG-AspSer) which correlates with its stronger destabilizing effect. Given that the molecular difference between the SerAsp and AspSer peptides is fairly minor, our work highlights the sensitivity of dipeptide sequences on protein-IL effects. While the specific nature of the protein-IL interactions is difficult to ascertain with the current experimental results, it stands to reason that the interactions involve specific portions of the protein and provide motivation for developing tailored, protein-specific ILs for various biomedical and bioengineering applications.

Declaration of competing interest

The authors declare that they have no known competing financial interests or personal relationships that could have appeared to influence the work reported in this paper.

Data availability

Data will be made available on request.

Acknowledgements

This work was supported by NSF grant DMR-1904797. The authors would like to acknowledge Gurvir Singh for experimental assistance.

Appendix A. Supplementary data

Supplementary data to this article can be found online at https://doi.org/10.1016/j.bbrep.2022.101242.

References

[1] K. Dong, X. Liu, H. Dong, X. Zhang, S. Zhang, Multiscale studies on ionic liquids, Chem. Rev. 117 (2017) 6636–6695, https://doi.org/10.1021/acs.chemrev.6b00776.
[2] M. Watanabe, M.L. Thomas, S. Zhang, K. Ueno, T. Yasuda, K. Dokko, Application of ionic liquids to energy storage and conversion materials and devices, Chem. Rev. 117 (2017) 7190–7239, https://doi.org/10.1021/acs.chemrev.6b00504.
[3] K. Fujita, D.R. MacFarlane, M. Forsyth, Protein solubilising and stabilising ionic liquids, Chem. Commun. (2005) 4804–4806, https://doi.org/10.1039/B508238B.
[4] D.S. Silvester, Recent advances in the use of ionic liquids for electrochemical sensing, Analyst 136 (2011) 4871–4882, https://doi.org/10.1039/C1AN15699C.
[5] P. Wasserscheid, W. Keim, Ionic liquids—new “solutions” for transition metal catalysis, Angew. Chem. Int. Ed. 39 (2000) 3772–3789, https://doi.org/10.1002/1521-3773(20001103)39:21<3772::AID-ANIE3772>3.0.CO, 2-5.
[6] K.S. Egorova, E.G. Gordeev, V.P. Ananikov, Biological activity of ionic liquids and their application in pharmaceutics and medicine, Chem. Rev. 117 (2017) 7132–7189, https://doi.org/10.1021/acs.chemrev.6b00562.
[7] A.A.M. Elgharbawy, M. Moniruzzaman, M. Goto, Recent advances of enzymatic reactions in ionic liquids: Part II, Biochem. Eng. J. 154 (2020), https://doi.org/10.1016/j.bej.2019.107426, 107426.
[8] Z. Sidat, T. Marimuthu, P. Kumar, L.C. du Toit, P.P.D. Kondiah, Y.E. Choonara, V. Pillay, Ionic liquids as potential and synergistic permeation enhancers for transdermal drug delivery, Pharmaceutics 11 (2019), https://doi.org/10.3390/pharmaceutics11020096.
[9] K. Cook, K. Tarnawsky, J.A. Swinton, D.D. Yang, S.A. Senetra, A.G. Caputo, R. B. Carone, D.T. Vaden, Correlating lipid membrane permeabilities of imidazolium ionic liquids with their cytotoxicities on yeast, bacterial, and mammalian cells, Biomolecules 9 (2019), https://doi.org/10.3390/biom9060251.
[10] S.-K. Ruokonen, C. Sanwald, A. Robciuc, S. Hietala, A.H. Rantamäki, J. Witos, A.W. T. King, M. Lämmerhofer, S.K. Wiedmer, Correlation between ionic liquid cytotoxicity and liposome–ionic liquid interactions, Chem. Eur J. 24 (2018) 2669–2680, https://doi.org/10.1002/chem.201704924.
[11] R. Caparica, A. Julio, J.P. Mota, C.R.T.S. de Almeida, Applicability of ionic liquids in topical drug delivery systems: a mini review, Int. J. Clin. Pharmacol. Res. 4 (2018) 555649.
[12] M. Zakrewski, K.S. Lovejoy, T.L. Kern, T.E. Miller, V. Le, A. Nagy, A.M. Goumas, R. S. Iyer, R.E. Del Sesto, A.T. Koppisch, D.T. Fox, S. Mitragotri, Ionic liquids as a class of materials for transdermal delivery and pathogen neutralization, Proc. Natl. Acad. Sci. U.S.A. 111 (2014) 13313–13318.
[13] G.S. Lim, J. Zidar, D.W. Cheong, S. Jaenicke, M. Klahn, Impact of ionic liquids in aqueous solution on bacterial plasma membranes studied with molecular dynamics simulations, J. Phys. Chem. B 118 (2014) 10444–10459, https://doi.org/10.1021/jp5060952.
[14] G. Liu, Applications of ionic liquids in biomedicine, biophys, Rev. Let. 7 (2012) 121–134.
[15] J. Stanton, Y. Xue, P. Pandher, L. Malek, T. Brown, X. Hu, D. Salas-de la Cruz, Impact of ionic liquid type on the structure, morphology and properties of silk-cellulose biocomposite materials, Int. J. Biol. Macromol. 108 (2018) 333–341, https://doi.org/10.1016/j.ijbiomac.2017.11.137.
[16] A.Y. Patel, K.S. Jonnalagadda, N. Paradis, T.D. Vaden, C. Wu, G.A. Caputo, Effects of ionic liquids on metalloproteins, Molecules 26 (2021), https://doi.org/10.3390/molecules26020514.
[17] L. Bui-Le, C.J. Clarke, A. Bröhl, A.P.S. Brogan, J.A.J. Arpino, K.M. Polizzi, J. P. Hallett, Revealing the complexity of ionic liquid–protein interactions through a multi-technique investigation, Commun. Chem. 3 (2020) 55, https://doi.org/10.1038/s42004-020-0302-5.
[18] L. Hao, W. Xing, S. Jianliang, C. Shicheng, Stimulation of laccase biocatalysis in ionic liquids: a review on recent progress, Curr. Protein Pept. Sci. 18 (2017) 1–12, https://doi.org/10.2174/1389203718666161122110647.
[19] E.M. Nordwald, G.S. Armstrong, J.L. Kaar, NMR-guided rational engineering of an ionic-liquid-tolerant lipase, ACS Catal. 4 (2014) 4057–4064.
[20] E.M. Nordwald, J.L. Kaar, Mediating electrostatic binding of 1-Butyl-3-methylimidazolium chloride to enzyme surfaces improves conformational stability, J. Phys. Chem. B 117 (2013) 8977–8986.
[21] C. Schroder, Proteins in ionic liquids: current status of experiments and simulations, Top. Curr. Chem. 375 (2017) 25, https://doi.org/10.1007/s41061-017-0110-2.
[22] S. Jens, Aqueous ionic liquids and their effects on protein structures: an overview on recent theoretical and experimental results, J. Phys. Condens. Matter 29 (2017) 233001.
[23] A.M. Figueiredo, J. Sardinha, G.R. Moore, E.J. Cabrita, Protein destabilisation in ionic liquids: the role of preferential interactions in denaturation, Phys. Chem. Chem. Phys. 15 (2013) 19632–19643.
[24] A. Schindl, M.L. Hagen, S. Muzammal, H.A.D. Gunasekera, A.K. Croft, Proteins in ionic liquids: reactions, applications, and futures, Front. Chem. 7 (2019), https://doi.org/10.3389/fchem.2019.00347.
[25] M. Reslan, V. Kayser, Ionic liquids as biocompatible stabilizers of proteins, Biophys. Rev. 10 (2018) 781–793, https://doi.org/10.1007/s12551-018-0407-6.
[26] H. Ohno, K. Fukumoto, Amino acid ionic liquids, Acc. Chem. Res. 40 (2007) 1122–1129.
[27] K. Fukumoto, M. Yoshizawa, H. Ohno, Room temperature ionic liquids from 20 natural amino acids, J. Am. Chem. Soc. 127 (2005) 2398–2399.
[28] P. Ossowicz, J. Klebeko, B. Roman, E. Janus, Z. Rozwadowski, The relationship between the structure and properties of amino acid ionic liquids, Molecules 24 (2019) 3252, https://doi.org/10.3390/molecules24183252.
[29] A.R. Shaikh, M. Ashraf, T. AlMayef, M. Chawla, A. Poater, L. Cavallo, Amino acid ionic liquids as potential candidates for CO2 capture: combined density functional theory and molecular dynamics simulations, Chem. Phys. Lett. 745 (2020) 137239, https://doi.org/10.1016/j.cplett.2020.137239.
[30] X. Ding, Y. Wang, Q. Zeng, J. Chen, Y. Huang, K. Xu, Design of functional guanidinium ionic liquid aqueous two-phase systems for the efficient purification of protein, Anal. Chem. Acta 815 (2014) 22–32.
[31] I. DeStefano, G. DeStefano, N.J. Paradis, R. Patel, A.K. Clark, H. Gogoj, G. Singh, K. S. Jonnalagadda, A.Y. Patel, C. Wu, G.A. Caputo, T.D. Vaden, Thermodynamic destabilization of azurin by four different tetramethylguanidinium amino acid ionic liquids, Int. J. Biol. Macromol. 180 (2021) 355–364, https://doi.org/10.1016/j.ijbiomac.2021.03.090.
[32] S. Sarkar, P. Rajdev, P.C. Singh, Hydrogen bonding of ionic liquids in the groove region of DNA controls the extent of its stabilization: synthesis, spectroscopic and simulation studies, Phys. Chem. Chem. Phys. 22 (2020) 15582–15591, https://doi.org/10.1039/D0CP01548B.
[33] K.L. Borrell, C. Cancglin, B.L. Stinger, K.G. DeFrates, G.A. Caputo, C. Wu, T. D. Vaden, An experimental and molecular dynamics study of red fluorescent protein mCherry in novel aqueous amino acid ionic liquids, J. Phys. Chem. B 121 (2017) 4823–4832.
[34] Z. Zhang, Y. Nie, Q. Zhang, X. Liu, W. Tu, X. Zhang, S. Zhang, Quantitative change in disulfide bonds and microstructure variation of regenerated wool keratin from various ionic liquids, ACS Sustain. Chem. Eng. 5 (2017) 2614–2622, https://doi.org/10.1021/acssuschemeng.6b02963.
[35] B. Iqbal, N. Muhammad, A. Jamal, P. Ahmad, Z.U.H. Khan, A. Rahim, A.S. Khan, G. Gonfa, J. Iqbal, I.U. Rehman, An application of ionic liquid for preparation of homogeneous collagen and alginate hydrogels for skin dressing, J. Mol. Liq. 243 (2017) 720–725, https://doi.org/10.1016/j.molliq.2017.08.101.
[36] N. Goujon, X. Wang, R. Rajkowa, N. Byrne, Regenerated silk fibroin using protic ionic liquids solvents: towards an all-ionic-liquid process for producing silk with tunable properties, Chem. Commun. 48 (2012) 1278–1280, https://doi.org/10.1039/C2CC17143K.
[37] H. Liu, L. Zhu, M. Bocola, N. Chen, A.C. Spiess, U. Schwaneberg, Directed laccase evolution for improved ionic liquid resistance, Green Chem. 15 (2013) 1348–1355, https://doi.org/10.1039/C3GC36899H.
[38] E.C. Wijaya, F. Separovic, C.J. Drummond, T.L. Greaves, Stability and activity of lysozyme in stoichiometric and non-stoichiometric protic ionic liquid (PIL)-water systems, J. Chem. Phys. 148 (2018) 193838, https://doi.org/10.1063/1.5010055.
[39] O.C. Fiebig, E. Mancini, G. Caputo, T.D. Vaden, Quantitative evaluation of myoglobin unfolding in the presence of guanidinium hydrochloride and ionic liquids in solution, J. Phys. Chem. B 118 (2014) 406–412.
[40] A. Acharyya, D. DiGiuseppi, B.L. Stinger, R. Schweitzer-Stenner, T.D. Vaden, Structural destabilization of azurin by imidazolium chloride ionic liquids in

aqueous solution, J. Phys. Chem. B 123 (2019) 6933–6945, https://doi.org/10.1021/acs.jpcb.9b04113.
[41] F. De Rienzo, R.R. Gabdoulline, M.C. Menziani, R.C. Wade, Blue copper proteins: a comparative analysis of their molecular interaction properties, Protein Sci. 9 (2000) 1439–1454, https://doi.org/10.1110/ps.9.8.1439.
[42] J. Yang, L. Feng, S. Pi, D. Cui, F. Ma, H.-p. Zhao, A. Li, A critical review of aerobic denitrification: insights into the intracellular electron transfer, Sci. Total Environ. 731 (2020) 139080, https://doi.org/10.1016/j.scitotenv.2020.139080.
[43] S. Kiani, K. Kujala, J.T. Pulkkinen, S.L. Aalto, S. Suurnäkki, T. Kiuru, M. Tiirola, B. Kløve, A.-K. Ronkanen, Enhanced nitrogen removal of low carbon wastewater in denitrification bioreactors by utilizing industrial waste toward circular economy, J. Clean. Prod. 254 (2020), https://doi.org/10.1016/j.jclepro.2020.119973, 119973.
[44] M. van de Kamp, M.C. Silvestrini, M. Brunori, J. Van Beeumen, F.C. Hali, G. W. Canters, Involvement of the hydrophobic patch of azurin in the electron-transfer reactions with cytochrome c551 and nitrite reductase, Eur. J. Biochem. 194 (1990) 109–118, https://doi.org/10.1111/j.1432-1033.1990.tb19434.x.
[45] E.M. Laming, A.P. McGrath, J.M. Guss, U. Kappler, M.J. Maher, The X-ray crystal structure of a pseudoazurin from Sinorhizobium meliloti, J. Inorg. Biochem. 115 (2012) 148–154, https://doi.org/10.1016/j.jinorgbio.2012.04.005.
[46] A.G. Szabo, T.M. Stepanik, D.M. Wayner, N.M. Young, Conformational heterogeneity of the copper binding site in azurin. A time-resolved fluorescence study, Biophys. J. 41 (1983) 233–244, https://doi.org/10.1016/S0006-3495(83)84433-6.
[47] S.J. Kroes, G.W. Canters, G. Gilardi, A. van Hoek, A.J.W.G. Visser, Time-Resolved fluorescence study of azurin variants: conformational heterogeneity and tryptophan mobility, Biophys. J. 75 (1998) 2441–2450, https://doi.org/10.1016/S0006-3495(98)77688-X.
[48] A.B.T. Ghisaidoobe, S.J. Chung, Intrinsic tryptophan fluorescence in the detection and analysis of proteins: a focus on förster resonance energy transfer techniques, Int. J. Mol. Sci. 15 (2014), https://doi.org/10.3390/ijms151222518.
[49] E. Terasaka, K. Yamada, P.-H. Wang, K. Hosokawa, R. Yamagiwa, K. Matsumoto, S. Ishii, T. Mori, K. Yagi, H. Sawai, H. Arai, H. Sugimoto, Y. Sugita, Y. Shiro, T. Tosha, Dynamics of nitric oxide controlled by protein complex in bacterial system, Proc. Natl. Acad. Sci. Unit. States Am. 114 (2017) 9888.
[50] S. Horrell, D. Kekilli, R.W. Strange, M.A. Hough, Recent structural insights into the function of copper nitrite reductases, Metallomics : Integrated Biometal Sci. 9 (2017) 1470–1482, https://doi.org/10.1039/c7mt00146k.
[51] H.D. Monteith, T.R. Bridle, P.M. Sutton, Industrial waste carbon sources for biological denitrification, in: S.H. Jenkins (Ed.), Water Pollution Research and Development, Pergamon, 1981, pp. 127–141.
[52] N. Suri, Y. Zhang, L.M. Gieg, M.C. Ryan, Denitrification biokinetics: towards optimization for industrial applications, Front. Microbiol. 12 (2021) 795.
[53] C. La Rosa, D. Milardi, D. Grasso, R. Guzzi, L. Sportelli, Thermodynamics of the thermal unfolding of azurin, J. Phys. Chem. 99 (1995) 14864–14870, https://doi.org/10.1021/j100040a041.
[54] A. Kumar, M. Bisht, P. Venkatesu, Biocompatibility of ionic liquids towards protein stability: a comprehensive overview on the current understanding and their implications, Int. J. Biol. Macromol. 96 (2017) 611–651, https://doi.org/10.1016/j.ijbiomac.2016.12.005.
[55] R. Patel, M. Kumari, A.B. Khan, Recent advances in the applications of ionic liquids in protein stability and activity: a review, Appl. Biochem. Biotechnol. 172 (2014) 3701–3720, https://doi.org/10.1007/s12010-014-0813-6.
[56] G.A. Caputo, E. London, Position and ionization state of Asp in the core of membrane-inserted α helices control both the equilibrium between transmembrane and nontransmembrane helix topography and transmembrane helix positioning, Biochemistry 43 (2004) 8794–8806, https://doi.org/10.1021/bi049696p.
[57] V.V. Khrustalev, V.V. Poboinev, A.N. Stojarov, T.A. Khrustaleva, Microenvironment of tryptophan residues in proteins of four structural classes: applications for fluorescence and circular dichroism spectroscopy, Eur. Biophys. J. 48 (2019) 523–537, https://doi.org/10.1007/s00249-019-01377-0.
[58] A.W. McMillan, B.L. Kier, I. Shu, A. Byrne, N.H. Andersen, W.W. Parson, Fluorescence of tryptophan in designed hairpin and trp-cage miniproteins: measurements of fluorescence yields and calculations by quantum mechanical molecular dynamics simulations, J. Phys. Chem. B 117 (2013) 1790–1809, https://doi.org/10.1021/jp3097378.